Published in final edited form as:
Oncogene. 2008 December 11; 27(58): 7260–7273. doi:10.1038/onc.2008.328.

Soluble monomeric EphrinA1 is released from tumor cells and is a functional ligand for the EphA2 receptor

J Wykosky[1], **E Palma**[1,2], **DM Gibo**[1], **S Ringler**[3], **CP Turner**[3], and **W Debinski**[1,2,4]

[1]Department of Neurosurgery, Brain Tumor Center of Excellence, Wake Forest University School of Medicine, Comprehensive Cancer Center, Winston-Salem, NC, USA

[2]Department of Radiation Oncology, Brain Tumor Center of Excellence, Wake Forest University School of Medicine, Comprehensive Cancer Center, Winston-Salem, NC, USA

[3]Department of Neurobiology and Anatomy, Brain Tumor Center of Excellence, Wake Forest University School of Medicine, Comprehensive Cancer Center, Winston-Salem, NC, USA

[4]Department of Cancer Biology, Brain Tumor Center of Excellence, Wake Forest University School of Medicine, Comprehensive Cancer Center, Winston-Salem, NC, USA

Abstract

The ephrinA1 ligand exerts antioncogenic effects in tumor cells through activation and downregulation of the EphA2 receptor and has been described as a membrane-anchored protein requiring clustering for function. However, while investigating the ephrinA1/EphA2 system in the pathobiology of glioblastoma multiforme (GBM), we uncovered that ephrinA1 is released from GBM and breast adenocarcinoma cells as a soluble, monomeric protein and is a functional form of the ligand in this state. Conditioned media containing a soluble monomer of ephrinA1 caused EphA2 internalization and downregulation, dramatic alteration of cell morphology and suppression of the Ras–MAPK pathway. Moreover, soluble monomeric ephrinA1 was functional in a physiological context, eliciting collapse of embryonic neuronal growth cones. We also found that ephrinA1 is cleaved from the plasma membrane of GBM cells, an event which involves the action of a metalloprotease. Thus, the ephrinA1 ligand can, indeed, function as a soluble monomer and may act in a paracrine manner on the EphA2 receptor without the need for juxtacrine interactions. These findings have important implications for further deciphering the function of these proteins in pathology and physiology, as well as for the design of ephrinA1-based EphA2-targeted antitumor therapeutics.

Keywords

ephrinA1; EphA2; glioblastoma; monomer; soluble

Introduction

The ephrins comprise a family of ligands for the Eph receptor tyrosine kinases that have been characterized as glycosyl phosphatidyl inositol (GPI)-anchored (ephrinA) or transmembrane (ephrinB) cell surface proteins (Davis *et al.*, 1994). Ephrins have important

Correspondence: Dr W Debinski, Director, Brain Tumor Center of Excellence, Departments of Neurosurgery, Radiation Oncology, and Cancer Biology, Comprehensive Cancer Center of Wake Forest University, Wake Forest University School of Medicine, Medical Center Boulevard, Winston-Salem, NC 27157, USA. debinski@wfubmc.edu.

Supplementary Information accompanies the paper on the Oncogene website (http://www.nature.com/onc)

functions in the developing central nervous system (Drescher *et al.*, 1995; Nakamoto *et al.*, 1996; Knoll and Drescher, 2002; Rashid *et al.*, 2005) and in the formation and organization of the vasculature (McBride and Ruiz, 1998; Wang *et al.*, 1998). Ephrin/Ephs have also been implicated in the development and progression of malignancy. Specifically, the EphA2 receptor is overexpressed and functionally important in solid tumors of the breast (Zelinski *et al.*, 2001; Wu *et al.*, 2004), prostate (Walker-Daniels *et al.*, 1999; Zeng *et al.*, 2003), ovary (Thaker *et al.*, 2004) and several others (Kinch and Carles-Kinch, 2003). We have found that EphA2 is abundantly and specifically overexpressed in glioblastoma multiforme (GBM), the most common adult primary malignant brain tumor of dismal prognosis (Wykosky *et al.*, 2005).

EphrinA1, a ligand for EphA2, is present at low levels in GBM (Wykosky *et al.*, 2005) and possesses tumor-suppressing properties in this and other solid tumors (Noblitt *et al.*, 2004; Duxbury *et al.*, 2004b; Guo *et al.*, 2006). A similar pattern of differential ephrinA1/EphA2 expression was found in breast cancer cells (Macrae *et al.*, 2005). Interestingly, ephrinA1 is also present in the vasculature of some tumors (Ogawa *et al.*, 2000) and was shown to have a critical function in inducing tumor angiogenesis through EphA2 expressed on endothelial cells (Brantley-Sieders *et al.*, 2006). EphrinA1 was originally identified as a tumor necrosis factor-α-inducible gene product in endothelial cells, and the C terminus has high structural similarity to proteins that undergo GPI-linkage to the plasma membrane (Ferguson and Williams, 1988; Holzman *et al.*, 1990). However, it was only later demonstrated that the ligand exists as a GPI-anchored protein by its ability to be released upon treatment with phosphatidylinositol-specific phospholipase C (PI-PLC) (Shao *et al.*, 1995). In addition, soluble ephrinA1 induced tyrosine phosphorylation of the EphA5 receptor only when artificially clustered by antibodies (Davis *et al.*, 1994). These observations, coupled with structural studies on some specific ephrin/Eph complexes (Himanen *et al.*, 2001; Toth *et al.*, 2001), gave rise to the notion that ephrin-mediated activation of Eph receptors requires cell–cell contact or oligomerization of soluble ephrins, for example, in the form of fusion ephrin-IgG-Fc proteins (Stein *et al.*, 1998). Hence, membrane-anchored ephrinA1 is widely considered the endogenous, functional form of the ligand (Beckmann *et al.*, 1994; Xu and Wilkinson, 1997; Kullander and Klein, 2002; Pasquale, 2005). The important physiological functions of ephrinA1 thus appear to be largely dependent on cell–cell contact (Pandey *et al.*, 1995; Daniel *et al.*, 1996; McBride and Ruiz, 1998; Cheng *et al.*, 2002; Marquardt *et al.*, 2005).

On the basis of our previous findings that ephrinA1 elicits a tumor-suppressing function in GBM, we became interested in exploring the form of ephrinA1, which exerts an antioncogenic effect. We are providing the first direct evidence that ephrinA1 is released from tumor cells as a soluble monomer that is capable of eliciting cellular responses in cancer cells that are not dependent on juxtacrine interactions.

Results

EphrinA1 overexpression downregulates EphA2 and suppresses malignant properties of GBM cells

U-251MG GBM cells, which naturally overexpress EphA2 with low levels of ephrinA1, were transfected with full-length human *ephrinA1*. [*ephrinA1*](+) clones 4, 7 and 12 exhibited a dramatic decrease in EphA2 protein when compared to controls (Figure 1a). Breast cancer cells that endogenously overexpress ephrinA1 had similarly low levels of EphA2 (Figure 1a). These findings were confirmed using confocal microscopy (Figure 1b). Hence, overexpression of ectopic ephrinA1 coincides with a marked decrease in EphA2 protein in GBM cells.

We next investigated possible functional consequences of ectopic ephrinA1 in GBM cells. U-251[*ephrinA1*](+) cells exhibited a significant defect in both migration and proliferation compared to controls (Figures 1c and d). Moreover, overexpression of ephrinA1 conferred a marked reduction in anchorage-independent growth similar to that observed upon treatment with ephrinA1-Fc, a soluble recombinant homodimeric ligand (Figure 1e). Thus, U-251[*ephrinA1*](+) cells exhibit downregulation of EphA2 and suppression of several of the malignant properties of GBM cells.

EphrinA1 is released from GBM and breast cancer cells as a soluble monomeric protein

Next, to investigate whether the decreased levels of EphA2 found in confluent monolayers of U-251[*ephrinA1*](+) and SK-Br-3 cells (Figure 1a) are dependent on cell–cell contact, cells were plated at low or high density (Supplementary Figure 1). To our surprise, the downregulation of EphA2 persisted in cells plated at low density (Figure 2a), indicating that ectopically and endogenously overexpressed ephrinA1 elicits downregulation of EphA2 that is not dependent on extensive cell–cell contact. This finding prompted us to hypothesize that ephrinA1 is released into the media of these cells in a functional form.

Thus, we examined the presence of ephrinA1 in conditioned media. Immunoreactive ephrinA1 was abundant in U-251[*ephrinA1*](+), SK-Br-3, T47D and ZR-75-1 cell media, but not in controls (Figure 2b). We also performed western blotting under non-reducing conditions, in which we still detected only a single 25-kDa immunoreactive band corresponding to ephrinA1 (Figure 2c). In addition to being present in whole cell lysates and in the media, some of the protein was also localized to the plasma membrane. Immunoreactive ephrinA1 was readily detected in biotinylated plasma membrane proteins and had a molecular weight slightly larger than its counterparts both in the media and lysates; a difference in size is likely because of the addition of biotin (Figure 2d). The release of ephrinA1 into the media was time-dependent (Figure 2e).

To determine the exact form of soluble ephrinA1, gel filtration chromatography was performed using media from U-251[*ephrinA1*](+) cells. A single ~25 kDa ephrinA1 immunoreactive protein was found in the fractions at 62 through 67 ml (Figure 2f). The predicted molecular mass of ephrinA1 was 29 772 kDa. Importantly, no dimeric or oligomeric forms of the protein were detected. Thus, soluble ephrinA1 released from GBM cells exists in a monomeric form.

Soluble, monomeric ephrinA1 induces internalization and downregulation of EphA2

We next demonstrated that EphA2 was profoundly downregulated in U-251MG and A-172MG GBM cells treated with ephrinA1-conditioned media obtained from either U-251[*ephrinA1*](+) cells or SK-Br-3 cells (Figures 3a and b). The magnitude of EphA2 downregulation was similar when compared to homodimeric ephrinA1-Fc (Figure 3c). EphA2 remained suppressed for at least 24 h in the presence of ligands (Figure 3c). Interestingly, *ephA2* gene expression also prominently decreased in response to 2 h treatment with homodimeric ephrinA1-Fc or a monomer of ephrinA1 generated by factor XA cleavage of ephrinA1-Fc, and then rebounded to slightly over control levels after 24 h (Figure 3d).

To study in more detail the fate of EphA2 in response to soluble monomeric ephrinA1, parental U-251MG cells were treated with ephrinA1-conditioned media or ephrinA1-Fc and examined by confocal microscopy. EphA2 was localized to the plasma membrane in non-treated cells (Figure 3e; 0 h). EphrinA1-conditioned media treatment caused EphA2 to internalize and relocate from the plasma membrane to the cytoplasmic and perinuclear regions of cells after 2 h, followed by a gradual decrease in the receptor level at 4 and 8 h

(Figure 3e). By 24 h, little detectable EphA2 protein remained, which was also the case in cells treated with ephrinA1-Fc (Figure 3e).

Functional effects of soluble monomeric ephrinA1 in GBM cells and embryonic neurons

Next, we explored the ability of soluble monomeric ephrinA1 to elicit cell rounding (Miao *et al.*, 2000). Cells treated with conditioned media from three different U-251[*ephrinA1*](+) clones became distinctly rounded, retracting most or all processes within 2 h of treatment (Figure 4a and Supplementary Figure 2A). We also transfected U-251MG cells with N-terminal 6-histidine-tagged ephrinA1 (His-ephrinA1). His-ephrinA1 was released as a monomer from these cells and isolated from the media through Ni^{2+} affinity chromatography (Supplementary Figure 2B). Treatment of U-251MG cells with His-ephrinA1 monomer resulted in a change in cell morphology identical to that observed in response to ephrinA1-conditioned media.

Dimeric ephrinA1-Fc was shown to suppress signaling through the Ras–MAPK pathway and to cause attenuation of growth factor-induced phosphorylation of ERK (Miao *et al.*, 2001; Macrae *et al.*, 2005; Guo *et al.*, 2006). We found that 10 min following treatment with empty vector-conditioned media (Figure 4b, top), there was a profound increase in ERK phosphorylation, but this effect was abolished in cells treated with ephrinA1-conditioned media (Figure 4b, bottom). The stimulation of ERK phosphorylation is likely a result of growth factors present in the conditioned media, and suppression of this increase when ephrinA1 is present supports the ability of a soluble monomer of ephrinA1 to engage in a functional interaction with EphA2. We did observe a transient increase in phosphorylated ERK in response to ephrinA1-conditioned media at 4 h, which may be because of the fact that at this time point, the majority of EphA2 has already internalized and downregulated (Figures 3c and e), reflecting a temporary suppression of ERK phosphorylation (Figures 4b and c).

We next investigated the effect of a soluble monomer of ephrinA1 on the collapse of embryonic neuronal growth cones. E.18 rat cortical neurons were treated with purified monomeric ephrinA1 or dimeric ephrinA1-Fc, and both significantly induced neuronal growth cone collapse (Figure 4c). Staining for EphA2 revealed that these cells do, indeed, express the receptor (Supplementary Figure 2D). We observed a similar potent increase in the number of collapsed growth cones in response to treatment of neurons with ephrinA1-conditioned media and not with control-conditioned media (data not shown).

EphrinA1-Fc is biologically functional both as homodimer and monomer

To examine whether homodimeric ephrinA1-Fc can function in a monomeric form, ephrinA1-Fc was reduced and alkylated (Debinski *et al.*, 1992) (Figure 5a). Dimeric and monomeric ephrinA1-Fc induced tyrosine phosphorylation of EphA2 (Figure 5b). Furthermore, treatment of U-251MG cells with either form of ephrinA1-Fc resulted in cell rounding and loss of polarity (Supplementary Figure 3). Dimeric and monomeric ephrinA1-Fc were very effective in inhibiting the migration of U-251MG cells (Figure 5c). We also compared the effect of dimeric and monomeric ephrinA1-Fc in eliciting neuronal growth cone collapse. Treatment with ephrinA1-Fc in both forms resulted in a significant increase in collapsed neuronal growth cones (Figure 5d).

Specificity of the monomeric ephrin–Eph interaction

It is not known whether other monomeric ephrins can functionally interact with EphA2 or whether monomeric ephrinA1 can interact with other EphA receptors. Thus, monomeric ephrinA1 and ephrinA5 were generated by cleaving off the Fc fragments from ephrinA1-Fc and ephrinA5-Fc, respectively (Figure 6a). Homodimeric ephrinA1-Fc and ephrinA5-Fc

downregulated EphA2 as expected (Figure 6b). The monomeric cleavage products (ephrinA1-cl and ephrinA5-cl) downregulated EphA2 as well (Figure 6b).

We also tested the ability of dimeric and monomeric ephrinA1 to induce downregulation of other EphA receptors. In SNB-19 cells, treatment with ephrinA1-Fc marginally induced downregulation of EphA5 compared to EphA2, whereas monomeric ephrinA1-cl appeared to have no effect on EphA5, but did induce downregulation of EphA2 (Figure 6c). Interestingly, in U-373MG cells, EphA3 and EphA2 were both downregulated in response to treatment with either ephrinA1-Fc or ephrinA1-cl (Figure 6c). U-373MG cells express lower levels of EphA2 than SNB-19 and U-251MG cells (Wykosky *et al.*, 2007). Thus, the ability of monomeric ephrinA1 to functionally interact with other EphA receptors may depend on the specific preference of binding such that when less EphA2 is available, the ligand interacts with other EphA receptors more efficiently.

Mechanism of ephrinA1 release from GBM cells

We next investigated the mechanism whereby monomeric ephrinA1 is released from GBM cells. Treatment of U-251[*ephrinA1*](+) cells with PI-PLC resulted in the release of ephrinA1, confirming that ephrinA1 is a GPI-anchored protein in these cells (Figure 7a; +PI-PLC). However, ephrinA1 naturally released from U-251[*ephrinA1*](+) cells was smaller by ~2–3 kDa than that released by PI-PLC (Figure 7a). Furthermore, the amount of ephrinA1 released from cells that had previously been treated with PI-PLC to release GPI-anchored proteins was considerably less than those that had not (Figure 7a).

To examine protease(s) that may be involved in the cleavage of ephrinA1, U-251[*ephrinA1*](+) cells were grown in the presence or absence of GM-6001, a broad-spectrum, specific inhibitor of metalloproteases. GM-6001 diminished the release of soluble monomeric ephrinA1 from U-251[*ephrinA1*](+) cells compared to treatment with vehicle (Figure 7b), indicating that enzyme of this class is involved in the cleavage and release of ephrinA1.

Discussion

We have uncovered that ephrinA1, a ligand for the EphA2 receptor, is released as a functional, soluble, monomeric protein by proteolytic cleavage from the plasma membrane of cancer cells. Soluble monomeric ephrinA1 induces downregulation of EphA2, elicits profound changes in cancer cell morphology, attenuates serum-induced phosphorylation of ERK and impairs cell migration and anchorage-independent growth. In addition, a monomer of ephrinA1-Fc has the same effects on EphA2 and downstream oncogenic processes as its homodimeric counterpart. These data reveal that soluble, monomeric ephrinA1 is a functional ligand for EphA2 in GBM and likely to exist in such a form in other cancers. Moreover, monomeric ephrinA1 effectively augments neuronal growth cone collapse, suggesting that a soluble form of the ligand may be involved in modulating physiological processes as well.

EphrinA1 as a recombinant dimeric Fc-fusion protein (ephrinA1-Fc) induces phosphorylation and downregulation of the EphA2 oncoprotein (Carles-Kinch *et al.*, 2002; Walker-Daniels *et al.*, 2002; Duxbury *et al.*, 2004a; Wykosky *et al.*, 2005). The notion that Ephs and ephrins may not, in fact, require the formation of oligomeric complexes has recent precedence in a study which found that ephrinA5 can engage in a functional interaction with the EphB2 receptor in a 1:1 heterodimeric complex, both in crystal structures and in solution (Himanen *et al.*, 2004). Interestingly, it represents one of the few known instances of cross-talk between A and B class Ephs and ephrins, which was in fact cited as a possible explanation for the existence of the unexpected, functional 1:1 receptor/ligand complex (Himanen *et al.*, 2004).

Our findings demonstrate for the first time that ephrins have functional functions as soluble, monomeric factors in activating Ephs of their own class during cancer maintenance and/or progression as well as normal developmental/physiological processes. In support of this finding, 12-amino acid ephrinA1-mimetic peptides have the capacity to bind and activate EphA2 (Koolpe *et al.*, 2002). Moreover, another ephrin ligand, ephrinA4, has been found to be released by activated B lymphocytes (Aasheim *et al.*, 2000). Our experiments with ephrinA1 purified from conditioned media, and homodimeric ephrinA1-Fc reduced to a monomer, and the Factor XA cleavage product documented the functional activity of this ligand as a soluble protein not requiring covalent dimerization or oligomerization for function. This suggests that the ligand is capable of interacting with EphA2 in a manner that is not totally dependent on juxtacrine interactions. Moreover, our results demonstrating that soluble monomeric ephrinA1 is effective in eliciting collapse of neuronal growth cones support a role for this form of the protein in physiology, as ephrinA1-induced growth cone collapse during embryonic development has been previously documented (Meima *et al.*, 1997).

We found that the monomeric ephrinA5 induced downregulation of EphA2 in GBM cells. Furthermore, monomeric ephrinA1 downregulated other EphA receptors, but only in U-373MG cells. In fact, we also observed a decreased ability of the dimeric ephrinA1-Fc to induce downregulation of EphA5 in SNB-19 cells, but this ligand efficiently induced downregulation of EphA3 in U-373MG cells. Thus, the ability of monomeric ephrinA1 to functionally interact with other EphA receptors may depend on the specific preference of binding such that when less EphA2 is available, the ligand interacts with other EphA receptors.

Autocrine and paracrine factors released by normal brain cells and acting on tumor cells have a crucial function in tumor development, prognosis and response to therapies (Hoelzinger *et al.*, 2007). We present evidence that ephrinA1 may be one such factor, as it is expressed in the normal brain tissue (Wykosky *et al.*, 2005). It is also possible that soluble ephrinA1 is released from tumor cells in response to specific angiogenic cues in the tumor microenvironment, many of which induce the expression of metalloproteases (Zucker *et al.*, 1998; VanMeter *et al.*, 2001; Sweeney *et al.*, 2002; Chakraborti *et al.*, 2003; Zhang *et al.*, 2006), which we have shown to be involved in the cleavage and release of ephrinA1. The exact metalloprotease(s) involved in the cleavage of this protein and the potential involvement of proteases of other classes warrants further investigation, but likely candidates are those within the ADAM family of metalloprotease enzymes. These enzymes are involved in the ectodomain shedding of many cell surface proteins (Lee *et al.*, 2003; Higashiyama and Nanba, 2005; Huovila *et al.*, 2005; Sanderson *et al.*, 2006). ADAM-10 has been implicated in the cleavage of ephrinA2 as a way of terminating the ephrinA2–EphA3 interaction between two cells (Hattori *et al.*, 2000).

We have documented for the first time that soluble, monomeric ephrinA1 is a functional ligand for EphA2 in GBM and modulates processes relevant to the progression of malignancy as well as central nervous system development. Furthermore, we have shown that ephrinA1 is not dependent on juxtacrine interactions and can function in a paracrine manner. These findings will aid in deciphering the function of ephrinA1 and EphA2 in solid tumor progression. In addition, they will facilitate the design and allow for a wider application of ephrinA1-based therapeutics targeting the EphA2 receptor involving, among others, the use of simplified soluble recombinant proteins/peptides and viral gene therapy.

Materials and methods

Cell lines and cell culture

U-251MG, SNB-19, A-172MG, U-373MG and SK-Br-3 were obtained from ATCC (Manassas, VA, USA) and grown as recommended by the manufacturer. ZR-75-1 cells were obtained from the Cell and Virus Vector Core Laboratory at Wake Forest University, and T47D cells were a generous gift from Dr Darren Seals (Wake Forest); both were grown in RPMI with 10% fetal bovine serum.

Transfection experiments

DNA (5 μg; *ephrinA1* pcDNA, *His-ephrinA1* pcDNA or empty vector control) was transfected into cells growing in Opti-MEM (Invitrogen, Carlsbad, CA, USA) using LipofectAMINE 2000 (Invitrogen). After 24 h, Opti-MEM was replaced with growth medium containing 20% fetal bovine serum. After 24 h, cells were split into 100 mm^2 dishes and geneticin (800 μg/ml) was added to select clones. Individual clones were isolated and maintained in growth medium containing 200 μg/ml geneticin.

Western blotting and immunoprecipitation

Western blotting was performed as previously described (Wykosky *et al.*, 2005). Primary antibodies included rabbit polyclonal anti-EphrinA1 (1:200) and anti-EphA5 (Santa Cruz Biotechnology, Santa Cruz, CA, USA), anti-EphA3 (1 μg/ml) (Zymed, S. San Francisco, CA, USA), mouse monoclonal anti-EphA2 clone D7 (1:1000), anti-phosphotyrosine clone PY20 (1:1000), and anti-β-actin (1:50 000) (Sigma, St Louis, MO, USA), rabbit polyclonal anti-phospho-Erk (1:1000) and anti-total-Erk (1:1000) (Cell Signaling Technology Inc., Danvers, MA, USA). EphA2 immunoprecipitation was performed as previously described (Wykosky *et al.*, 2005). Immunoprecipitates were stored at −80 °C until separated by SDS–polyacrylamide gel electrophoresis for western blotting.

Immunofluorescence and confocal microscopy

Immunofluorescent staining was performed as described previously (Wykosky *et al.*, 2005). Primary antibodies anti-EphA2 (1:100) or anti-ephrinA1 (1:100) were incubated overnight at 4 °C. Secondary antibodies included donkey anti-rabbit rhodamine (1:200) (Jackson ImmunoResearch Laboratories Inc., West Grove, PA, USA) or goat anti-mouse IgG Oregon Green (1:200) (Molecular Probes, Eugene, OR, USA). Nuclei were visualized by staining with TO-PRO-3 iodide (1:1000) (Molecular Probes). Slides were mounted with Gel-Mount (Biomeda Corp., Foster City, CA, USA). Confocal microscopy analysis was performed using a Zeiss LSM 510 Laser Scanning Confocal Microscope with a × 63 lens, and images were processed with Zeiss LSM Image Browser software.

Anchorage-independent growth assay

Cells (2×10^3) were plated in six-well dishes in growth medium plus 0.35% Agar (Difco, Lawrence, KS, USA), on a base layer of growth medium plus 0.5% Agar. A volume of 1 μg/ml ephrinA1-Fc (R&D Systems, Minneapolis, MN, USA) added to cells was replenished with fresh media after 3 days. Colonies were counted and photographed at low power after 14 days. Clusters of colonies greater than ~50 cells were counted in 10 random fields at low power; each experimental condition or cell line was assayed in triplicate.

Proliferation assay

A total of 1000 cells were plated in a 96-well plate in quadruplicate for each cell line. After 48 h in culture, proliferation was measured using a colorimetric MTS (3-(4,5-dimethylthiazol-2-yl)-5-(3-carboxymethoxyphenyl)-2-(4-sulfophenyl)-2H-tetrazolium, inner

salt)/PMS (phenazine methasulfate) cell proliferation assay as recommended by the manufacturer (Promega, Madison, WI, USA). Cells were incubated with the MTS/PMS dye for 2–4 h, and absorbance was measured at 490 nm using a microplate reader.

Migration assay

Wounds were made in a confluent monolayer of cells with a sterile 200 μl tip and growth media containing monomeric or dimeric ephrinA1-Fc (1 μg/ml) was added. Phase contrast-microscopy pictures were taken of the same field at 0, 8 and 24 h. Distance of the wound in μM was measured in five places for each of three wounds for each treatment or cell type at each time point using ImagePro Plus software, and the percent wound closure over 24 h was calculated for graphical representation.

Conditioned media

Conditioned media was collected from subconfluent monolayers, centrifuged for 5 min at 1000 r.p.m., and supernatant used immediately to treat cells or for western blotting or stored at −20 °C until use. For treatment of cells with conditioned media, cells were seeded, grown overnight and the normal growth media was replaced with conditioned media (undiluted unless otherwise indicated) for the indicated times. For treatment of cells with SK-Br-3 conditioned media, media was concentrated 5 × before use with 10 000 MWCO Amicon Ultra centrifugal filter devices (Millipore, Billerica, MA, USA).

Gel filtration analysis

A volume of 250 ml of conditioned media was collected from serum-starved (48 h) subconfluent monolayers of U-251 [*ephrinA1*](+) 12 cells, concentrated to ~1 ml and phosphate-buffered saline (PBS) buffer-exchanged. The media was loaded by FPLC onto a HiPrep 16/60 Sephacryl S-200 gel filtration column (GE Healthcare, Piscataway, NJ, USA) precalibrated with conalbumin, ovalbumin, carbonic anhydrase and ribonuclease A from the protein gel filtration calibration kit (GE Healthcare). EphrinA1-conditioned media individual fractions were collected and western blotted and ephrinA1-containing fractions were pooled and concentrated.

EphrinA1-Fc homodimer reduction to a monomer

A concentration of 10 mM DTT (Acros Organics, Morris Plains, NJ, USA) was added to ephrinA1-Fc or IgG_1 isotype control for 15 min at 37 °C. A concentration of 20 mM Iodoacetamide (IA) (Sigma) was added at room temperature for 20 min. A concentration of 10 mM DTT was added again for 15 min at 37 °C. Reduced products were purified using Spin-OUT 12 000 Micro columns (Chemicon, Temecula, CA, USA).

Neuronal growth cone experiments

Primary neuronal cultures were prepared from the cortical lobes of embryonic day 18 Sprague–Dawley rat embryos as previously described (Turner *et al.*, 2002). EphrinA1-Fc, PBS or IgG_1 isotype control was added to cells 48 h into culture and incubated for 1 h at 37 °C. Cells were fixed, permeabilized and stained with rhodamine-phalloidin (Invitrogen) for 20 min at room temperature, washed, and coverslips were mounted onto glass slides using Vectashield Hard Set mounting media containing DAPI (Vector Labs, Burlingame, CA, USA). Images were captured using an Olympus IX70 Inverted System Microscope (Olympus, Melville, NY, USA) and Hamamatsu digital camera (Hamamatsu City, Japan) with IPLab 3.6.4 software (Scanalytics Inc., Fairfax, VA, USA). Image-Pro Plus v.5.1 software was used for image analysis. Collapsed growth cones (CGC) were categorized as having a shrunken lamellipodia with no filopodia, and counts were normalized to the number of DAPI-stained nuclei in the same field (CGC/DAPI).

Biotinylation of plasma membrane proteins and streptavidin immunoprecipitation

Cells were plated in 150 mm round dishes, grown until 95% confluent and collected using a cell scraper. Cells were pelleted, resuspended in 10 ml PBS and pelleted again. Pellet was resuspended in a final volume of 500 μl PBS and transferred to a microfuge tube. NHS-PEO_4 Biotin No-Weigh 2 mg per vial (Pierce, Rockford, IL, USA) was prepared by resuspending in 170 μl ultrapure water. A volume of 80 μl of biotin was added to each cell suspension and incubated at room temperature for 30 min. Cells were washed three times with 1 ml PBS/100 mM glycine. Pellet was resuspended in 540 μl RIPA protease inhibitor cocktail, incubated on ice for 30 min and lysate collected after centrifugation at 10 000 r.p.m. for 10 min. Biotinylated lysate was stored at −80 °C until use for immunoprecipitation with streptavidin. Immobilized streptavidin (Pierce) was washed with PBS/0.1% SDS three times, and ~500 μl biotinylated lysate was added to 100 μl packed beads. Reaction mixture was incubated at room temperature on a rotator for 1 h, after which beads were washed five times with 500 μl PBS/0.1% SDS. Beads were resuspended in 50 μl 3 × SDS sample buffer, heated at 100 °C for 5 min and centrifuged for 5 min at 1000 r.p.m. Supernatant was collected and stored at −80 °C until used.

PI-PLC treatment

A total of 400 000 cells were plated in 60 mm round dishes and grown overnight. Adherent cells were washed twice with PBS, and 0.5 U/ml of PI-PLC (MP Biomedicals, Santa Ana, CA, USA) was added. Cells were incubated with or without PI-PLC for 20 min at 4 °C on rocker, then buffer was collected from each plate and stored to assay for released proteins. Cells were then washed twice more with PBS and replenished with fresh growth media.

Factor XA cleavage

Recombinant ephrinA1-Fc and ephrinA5-Fc (R&D systems) were cleaved at a site in the peptidyl linker between the ligand and Fc using a Factor Xa cleavage/capture kit as per manufacturer's instructions (Novagen, San Diego, CA, USA). Fc fragments were captured by incubating the reaction mixture with Protein G Sepharose FF (Sigma) at 4 °C for 48 h.

Protease inhibitor experiments

After 24 h in culture, media from subconfluent U-251 [*ephrinA1*](+) cells in 60 mm dishes was replaced with fresh growth media plus 25 μM GM-6001 (BioMol International, Plymouth Meeting, PA, USA) or an equal volume of dimethylsulfoxide. After 18 h, conditioned media samples were collected.

Real-time PCR

U-251MG cells were treated with PBS, ephrinA1-Fc (R&D Systems) or monomeric ephrinA1 isolated by Factor XA cleavage. RNA was obtained using the RNeasy Kit (Qiagen, Valencia, CA, USA). A quantity of 850 ng of total RNA was used to prepare cDNA with the High Capacity RNA to cDNA Kit (Applied Biosystems, Foster City, CA). The *EphA2* transcript levels were studied with real-time quantitative PCR based on the TaqMan methodology using 7000 real-time PCR system (Applied Biosystems). Gene Expression Assays (Applied Biosystems) were used to quantify the target and control genes. These assays are mixtures of an unlabeled PCR primer and a Taqman MGB probe (6-FAM) at the 5′ end with a non-fluorescent quencher at the 3′ end, designed over an exon–exon boundary to specifically detect cDNA sequences. The assay identification numbers of the selected genes are Hs171656_m1 for EphA2 and Hs99999903_m1 for β-actin. The expression of β-actin was used to normalize the cDNA template. A quantity of 40 ng of cDNA, universal Taq-Man PCR master mix (Applied Biosystems) and Gene Expression Assay primers were combined in a final volume of 25 μl. The amplification reactions, in

triplicate, were performed as follows, using a 7500 real-time PCR system according to the manufacturer's instructions: 95 °C for 10 min followed by 40 cycles of 95 °C for 15 s, 60 °C for 1 min. Data were analysed by the comparative CT method.

Statistical analyses

Statistical significance was determined by one-way analysis of variance. If $P<0.05$, Bonferroni's multiple comparison test was used to determine pairwise significance in all cases with the exception of the neuronal growth cone analysis, in which Neuman–Keuls *post hoc* testing was used. Error bars represent mean ± s.e.m.

Supplementary Material

Refer to Web version on PubMed Central for supplementary material.

Acknowledgments

This study was supported by the NIH Grant 1 F31 NSO55533-01 to JW, NIH Grant 5 T32 CA113267-04 to Dr Mike Robbins (EP) and Brain Tumor Center of Excellence at Wake Forest University School of Medicine. We thank Dr Hannah Caldas and Ms Amanda Beauchamp for help with real-time PCR and Ms Carla Lema-Tome for preparing cortical neurons.

References

Aasheim HC, Munthe E, Funderud S, Smeland EB, Beiske K, Logtenberg T. A splice variant of human ephrin-A4 encodes a soluble molecule that is secreted by activated human B lymphocytes. Blood. 2000; 95:221–230. [PubMed: 10607706]

Beckmann MP, Cerretti DP, Baum P, Vanden Bos T, James L, Farrah T, et al. Molecular characterization of a family of ligands for eph-related tyrosine kinase receptors. EMBO J. 1994; 13:3757–3762. [PubMed: 8070404]

Brantley-Sieders DM, Fang WB, Hwang Y, Hicks D, Chen J. Ephrin-A1 facilitates mammary tumor metastasis through an angiogenesis-dependent mechanism mediated by EphA receptor and vascular endothelial growth factor in mice. Cancer Res. 2006; 66:10315–10324. [PubMed: 17079451]

Carles-Kinch K, Kilpatrick KE, Stewart JC, Kinch MS. Antibody targeting of the EphA2 tyrosine kinase inhibits malignant cell behavior. Cancer Res. 2002; 62:2840–2847. [PubMed: 12019162]

Chakraborti S, Mandal M, Das S, Mandal A, Chakraborti T. Regulation of matrix metalloproteinases: an overview. Mol Cell Biochem. 2003; 253:269–285. [PubMed: 14619979]

Cheng N, Brantley DM, Liu H, Lin Q, Enriquez M, Gale N, et al. Blockade of EphA receptor tyrosine kinase activation inhibits vascular endothelial cell growth factor-induced angiogenesis. Mol Cancer Res. 2002; 1:2–11. [PubMed: 12496364]

Daniel TO, Stein E, Cerretti DP, St John PL, Robert B, Abrahamson DR. ELK and LERK-2 in developing kidney and microvascular endothelial assembly. Kidney Int Suppl. 1996; 57:S73–S81. [PubMed: 8941926]

Davis S, Gale NW, Aldrich TH, Maisonpierre PC, Lhotak V, Pawson T, et al. Ligands for EPH-related receptor tyrosine kinases that require membrane attachment or clustering for activity. Science. 1994; 266:816–819. [PubMed: 7973638]

Debinski W, Karlsson B, Lindholm L, Siegall CB, Willingham MC, FitzGerald D, et al. Monoclonal antibody C242-Pseudomonas exotoxin A. A specific and potent immunotoxin with antitumor activity on a human colon cancer xenograft in nude mice. J Clin Invest. 1992; 90:405–411. [PubMed: 1644913]

Drescher U, Kremoser C, Handwerker C, Loschinger J, Noda M, Bonhoeffer F. In vitro guidance of retinal ganglion cell axons by RAGS, a 25 kDa tectal protein related to ligands for Eph receptor tyrosine kinases. Cell. 1995; 82:359–370. [PubMed: 7634326]

Duxbury MS, Ito H, Zinner MJ, Ashley SW, Whang EE. EphA2: a determinant of malignant cellular behavior and a potential therapeutic target in pancreatic adenocarcinoma. Oncogene. 2004a; 23:1448–1456. [PubMed: 14973554]

Duxbury MS, Ito H, Zinner MJ, Ashley SW, Whang EE. Ligation of EphA2 by Ephrin A1-Fc inhibits pancreatic adenocarcinoma cellular invasiveness. Biochem Biophys Res Commun. 2004b; 320:1096–1102. [PubMed: 15249202]

Ferguson MA, Williams AF. Cell-surface anchoring of proteins via glycosyl-phosphatidylinositol structures. Annu Rev Biochem. 1988; 57:285–320. [PubMed: 3052274]

Guo H, Miao H, Gerber L, Singh J, Denning MF, Gilliam AC, et al. Disruption of EphA2 receptor tyrosine kinase leads to increased susceptibility to carcinogenesis in mouse skin. Cancer Res. 2006; 66:7050–7058. [PubMed: 16849550]

Hattori M, Osterfield M, Flanagan JG. Regulated cleavage of a contact-mediated axon repellent. Science. 2000; 289:1360–1365. [PubMed: 10958785]

Higashiyama S, Nanba D. ADAM-mediated ectodomain shedding of HB-EGF in receptor cross-talk. Biochim Biophys Acta. 2005; 1751:110–117. [PubMed: 16054021]

Himanen JP, Chumley MJ, Lackmann M, Li C, Barton WA, Jeffrey PD, et al. Repelling class discrimination: ephrin-A5 binds to and activates EphB2 receptor signaling. Nat Neurosci. 2004; 7:501–509. [PubMed: 15107857]

Himanen JP, Rajashankar KR, Lackmann M, Cowan CA, Henkemeyer M, Nikolov DB. Crystal structure of an Eph receptor-ephrin complex. Nature. 2001; 414:933–938. [PubMed: 11780069]

Hoelzinger DB, Demuth T, Berens ME. Autocrine factors that sustain glioma invasion and paracrine biology in the brain microenvironment. J Natl Cancer Inst. 2007; 99:1583–1593. [PubMed: 17971532]

Holzman LB, Marks RM, Dixit VM. A novel immediate-early response gene of endothelium is induced by cytokines and encodes a secreted protein. Mol Cell Biol. 1990; 10:5830–5838. [PubMed: 2233719]

Huovila AP, Turner AJ, Pelto-Huikko M, Karkkainen I, Ortiz RM. Shedding light on ADAM metalloproteinases. Trends Biochem Sci. 2005; 30:413–422. [PubMed: 15949939]

Kinch MS, Carles-Kinch K. Overexpression and functional alterations of the EphA2 tyrosine kinase in cancer. Clin Exp Metastasis. 2003; 20:59–68. [PubMed: 12650608]

Knoll B, Drescher U. Ephrin-As as receptors in topographic projections. Trends Neurosci. 2002; 25:145–149. [PubMed: 11852146]

Koolpe M, Dail M, Pasquale EB. An ephrin mimetic peptide that selectively targets the EphA2 receptor. J Biol Chem. 2002; 277:46974–46979. [PubMed: 12351647]

Kullander K, Klein R. Mechanisms and functions of Eph and ephrin signalling. Nat Rev Mol Cell Biol. 2002; 3:475–486. [PubMed: 12094214]

Lee DC, Sunnarborg SW, Hinkle CL, Myers TJ, Stevenson MY, Russell WE, et al. TACE/ADAM17 processing of EGFR ligands indicates a role as a physiological convertase. Ann N Y Acad Sci. 2003; 995:22–38. [PubMed: 12814936]

Macrae M, Neve RM, Rodriguez-Viciana P, Haqq C, Yeh J, Chen C, et al. A conditional feedback loop regulates Ras activity through EphA2. Cancer Cell. 2005; 8:111–118. [PubMed: 16098464]

Marquardt T, Shirasaki R, Ghosh S, Andrews SE, Carter N, Hunter T, et al. Coexpressed EphA receptors and ephrin-A ligands mediate opposing actions on growth cone navigation from distinct membrane domains. Cell. 2005; 121:127–139. [PubMed: 15820684]

McBride JL, Ruiz JC. Ephrin-A1 is expressed at sites of vascular development in the mouse. Mech Dev. 1998; 77:201–204. [PubMed: 9831653]

Meima L, Kljavin IJ, Moran P, Shih A, Winslow JW, Caras IW. AL-1-induced growth cone collapse of rat cortical neurons is correlated with REK7 expression and rearrangement of the actin cytoskeleton. Eur J Neurosci. 1997; 9:177–188. [PubMed: 9042581]

Miao H, Burnett E, Kinch M, Simon E, Wang B. Activation of EphA2 kinase suppresses integrin function and causes focal-adhesion-kinase dephosphorylation. Nat Cell Biol. 2000; 2:62–69. [PubMed: 10655584]

Miao H, Wei BR, Peehl DM, Li Q, Alexandrou T, Schelling JR, et al. Activation of EphA receptor tyrosine kinase inhibits the Ras/MAPK pathway. Nat Cell Biol. 2001; 3:527–530. [PubMed: 11331884]

Nakamoto M, Cheng HJ, Friedman GC, McLaughlin T, Hansen MJ, Yoon CH, et al. Topographically specific effects of ELF-1 on retinal axon guidance in vitro and retinal axon mapping in vivo. Cell. 1996; 86:755–766. [PubMed: 8797822]

Noblitt LW, Bangari DS, Shukla S, Knapp DW, Mohammed S, Kinch MS, et al. Decreased tumorigenic potential of EphA2-overexpressing breast cancer cells following treatment with adenoviral vectors that express EphrinA1. Cancer Gene Ther. 2004; 11:757–766. [PubMed: 15359289]

Ogawa K, Pasqualini R, Lindberg RA, Kain R, Freeman AL, Pasquale EB. The ephrin-A1 ligand and its receptor, EphA2, are expressed during tumor neovascularization. Oncogene. 2000; 19:6043–6052. [PubMed: 11146556]

Pandey A, Shao H, Marks RM, Polverini PJ, Dixit VM. Role of B61, the ligand for the Eck receptor tyrosine kinase, in TNF-alpha-induced angiogenesis. Science. 1995; 268:567–569. [PubMed: 7536959]

Pasquale EB. Eph receptor signalling casts a wide net on cell behaviour. Nat Rev Mol Cell Biol. 2005; 6:462–475. [PubMed: 15928710]

Rashid T, Upton AL, Blentic A, Ciossek T, Knoll B, Thompson ID, et al. Opposing gradients of ephrin-As and EphA7 in the superior colliculus are essential for topographic mapping in the mammalian visual system. Neuron. 2005; 47:57–69. [PubMed: 15996548]

Sanderson MP, Dempsey PJ, Dunbar AJ. Control of ErbB signaling through metalloprotease mediated ectodomain shedding of EGF-like factors. Growth Factors. 2006; 24:121–136. [PubMed: 16801132]

Shao H, Pandey A, O'Shea KS, Seldin M, Dixit VM. Characterization of B61, the ligand for the Eck receptor protein-tyrosine kinase. J Biol Chem. 1995; 270:5636–5641. [PubMed: 7890684]

Stein E, Lane AA, Cerretti DP, Schoecklmann HO, Schroff AD, Van Etten RL, et al. Eph receptors discriminate specific ligand oligomers to determine alternative signaling complexes, attachment, and assembly responses. Genes Dev. 1998; 12:667–678. [PubMed: 9499402]

Sweeney P, Karashima T, Kim SJ, Kedar D, Mian B, Huang S, et al. Anti-vascular endothelial growth factor receptor 2 antibody reduces tumorigenicity and metastasis in orthotopic prostate cancer xenografts via induction of endothelial cell apoptosis and reduction of endothelial cell matrix metalloproteinase type 9 production. Clin Cancer Res. 2002; 8:2714–2724. [PubMed: 12171905]

Thaker PH, Deavers M, Celestino J, Thornton A, Fletcher MS, Landen CN, et al. EphA2 expression is associated with aggressive features in ovarian carcinoma. Clin Cancer Res. 2004; 10:5145–5150. [PubMed: 15297418]

Toth J, Cutforth T, Gelinas AD, Bethoney KA, Bard J, Harrison CJ. Crystal structure of an ephrin ectodomain. Dev Cell. 2001; 1:83–92. [PubMed: 11703926]

Turner CP, Pulciani D, Rivkees SA. Reduction in intracellular calcium levels induces injury in developing neurons. Exp Neurol. 2002; 178:21–32. [PubMed: 12460605]

VanMeter TE, Rooprai HK, Kibble MM, Fillmore HL, Broaddus WC, Pilkington GJ. The role of matrix metalloproteinase genes in glioma invasion: co-dependent and interactive proteolysis. J Neurooncol. 2001; 53:213–235. [PubMed: 11716072]

Walker-Daniels J, Coffman K, Azimi M, Rhim JS, Bostwick DG, Snyder P, et al. Overexpression of the EphA2 tyrosine kinase in prostate cancer. Prostate. 1999; 41:275–280. [PubMed: 10544301]

Walker-Daniels J, Riese DJ, Kinch MS. c-Cbl-dependent EphA2 protein degradation is induced by ligand binding. Mol Cancer Res. 2002; 1:79–87. [PubMed: 12496371]

Wang HU, Chen ZF, Anderson DJ. Molecular distinction and angiogenic interaction between embryonic arteries and veins revealed by ephrin-B2 and its receptor Eph-B4. Cell. 1998; 93:741–753. [PubMed: 9630219]

Wu Q, Suo Z, Risberg B, Karlsson MG, Villman K, Nesland JM. Expression of Ephb2 and Ephb4 in breast carcinoma. Pathol Oncol Res. 2004; 10:26–33. [PubMed: 15029258]

Wykosky J, Gibo DM, Debinski W. A novel, potent, and specific ephrinA1-based cytotoxin against EphA2 receptor expressing tumor cells. Mol Cancer Ther. 2007; 6:3208–3218. [PubMed: 18089715]

Wykosky J, Gibo DM, Stanton C, Debinski W. EphA2 as a novel molecular marker and target in glioblastoma multiforme. Mol Cancer Res. 2005; 3:541–551. [PubMed: 16254188]

Xu Q, Wilkinson DG. Eph-related receptors and their ligands: mediators of contact dependent cell interactions. J Mol Med. 1997; 75:576–586. [PubMed: 9297625]

Zelinski DP, Zantek ND, Stewart JC, Irizarry AR, Kinch MS. EphA2 overexpression causes tumorigenesis of mammary epithelial cells. Cancer Res. 2001; 61:2301–2306. [PubMed: 11280802]

Zeng G, Hu Z, Kinch MS, Pan CX, Flockhart DA, Kao C, et al. High-level expression of EphA2 receptor tyrosine kinase in prostatic intraepithelial neoplasia. Am J Pathol. 2003; 163:2271–2276. [PubMed: 14633601]

Zhang A, Meng L, Wang Q, Xi L, Chen G, Wang S, et al. Enhanced in vitro invasiveness of ovarian cancer cells through up-regulation of VEGF and induction of MMP-2. Oncol Rep. 2006; 15:831–836. [PubMed: 16525667]

Zucker S, Mirza H, Conner CE, Lorenz AF, Drews MH, Bahou WF, et al. Vascular endothelial growth factor induces tissue factor and matrix metalloproteinase production in endothelial cells: conversion of prothrombin to thrombin results in progelatinase A activation and cell proliferation. Int J Cancer. 1998; 75:780–786. [PubMed: 9495249]

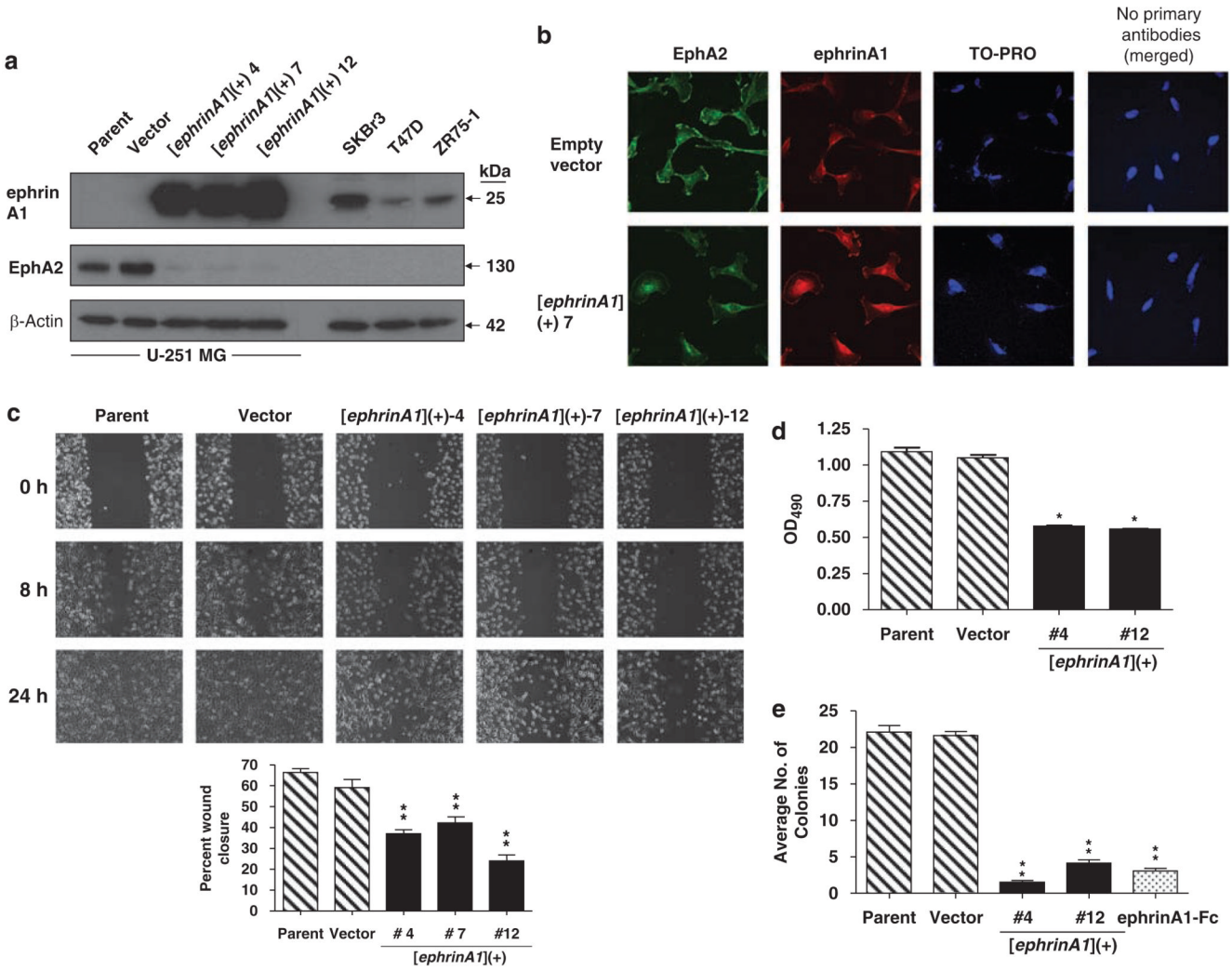

Figure 1.

Ectopic ephrinA1 decreases EphA2 and suppresses the malignant features of glioblastoma multiforme (GBM) cells. (**a**) Western blot analysis of ephrinA1 and EphA2 protein in confluent parent, empty-vector-transfected (vector), three clonally isolated lines of *ephrinA1*-transfected U-251MG GBM cells ([*ephrinA1*](+) 4, 7 and 12), and the breast carcinoma cell lines SK-Br-3, T47D and ZR-75-1. (**b**) Confocal microscopy of EphA2 and ephrinA1 in U-251 parent, empty-vector-transfected and [*ephrinA1*](+) 4, 7 and 12 cells. Nuclei were visualized with a fluorescent DNA-binding probe, TO-PRO. No primary antibody control images are merged for the two fluorescent secondary antibodies and TO-PRO. (**c**) Phase-contrast microscopy and quantitation of migration as percentage of wound closure at 24 h of U-251 parent, empty-vector-transfected and [*ephrinA1*](+) 4, 7 and 12 cells. (**d**) Proliferation of U-251 parent, empty-vector-transfected and [*ephrinA1*](+) 4 and 12 cells over a 48 h time period. (**e**) Anchorage-independent growth, measured by colony formation in soft agar, of U-251 parent, empty-vector-transfected, [*ephrinA1*](+) 4 and 12 and parent cells treated with 1 μg/ml ephrinA1-Fc. Colonies ≥75 cells were counted. **P*<0.005; ***P*<0.001.

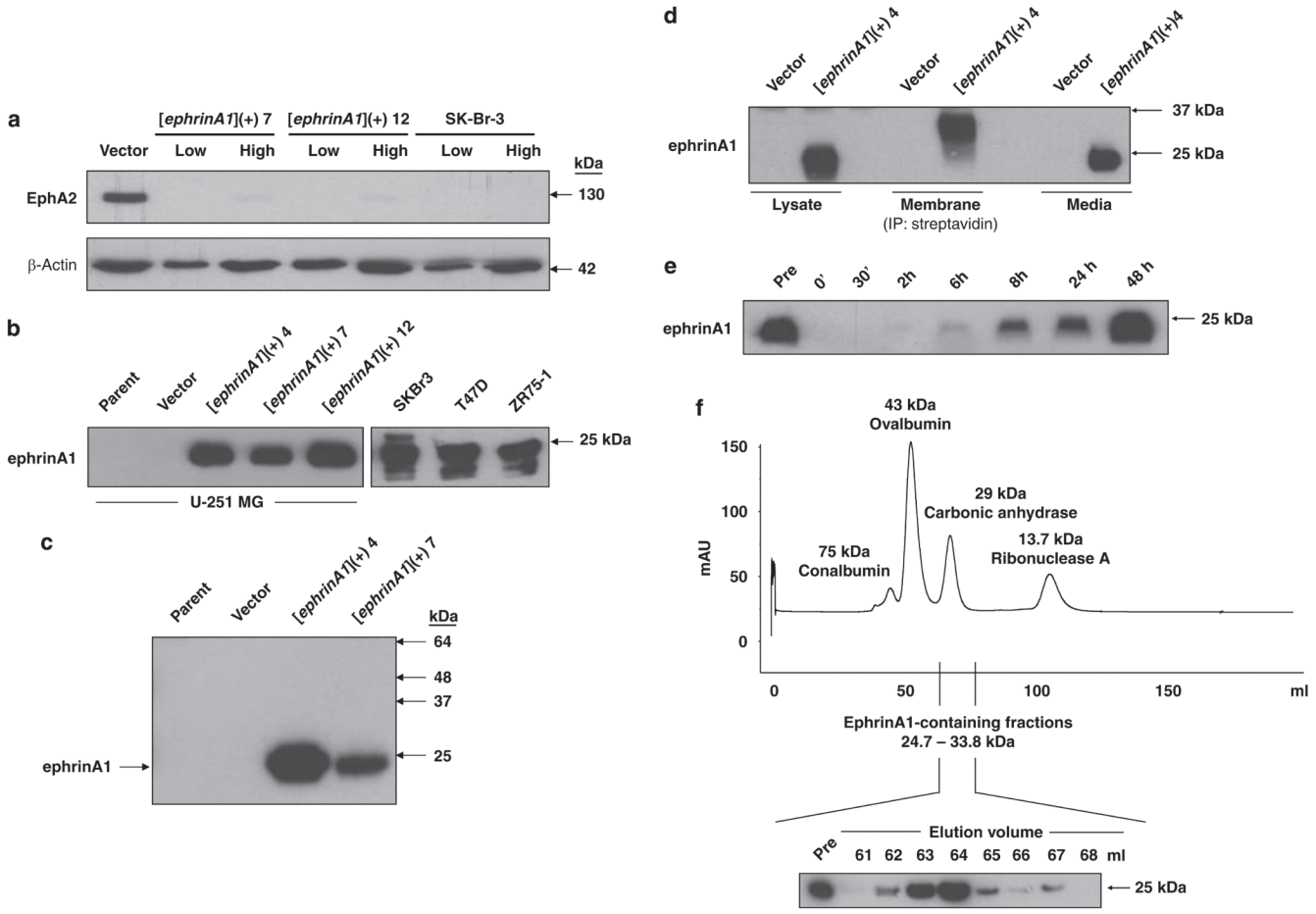

Figure 2.

EphrinA1 is released from glioblastoma multiforme (GBM) cells as a soluble, monomeric protein. (**a**) Western blot of EphA2 expression in empty-vector-transfected U-251MG cells, and in U-251[*ephrinA1*](+) and 12 and SK-Br-3 cells at low or high density. (**b**) Western blot, under reducing conditions, of ephrinA1 in conditioned media obtained from parental U-251MG, empty-vector-transfected U-251[*ephrinA1*](+) 4, 7 and 12, SK-Br-3, T47D and ZR-75-1 cells. SK-Br-3, T47D and ZR-75-1 samples were exposed three times longer than U-251 samples during western blotting development. (**c**) Western blot under non-reducing conditions of ephrinA1 presence in conditioned media obtained from parental U-251MG, empty-vector-transfected and U-251[*ephrinA1*](+) 4 and 7 cells. (**d**) Western blot analysis of ephrinA1 expression in whole cell lysates, plasma membrane and conditioned media of U-251 empty-vector-transfected and [*ephrinA1*](+) 12 cells. Plasma membrane proteins were isolated by biotinylation followed by immunoprecipitation with streptavidin-coated agarose beads. (**e**) Time course of soluble ephrinA1 release into the media of U-251[*ephrinA1*](+) 12 cells. Pre, media sample collected after cells were in culture for 24 h before the start of time course, for which cells were washed with PBS, fresh growth media was added, and samples of media collected at the indicated times and subject to analysis by western blotting. (**f**) FPLC chromatograph from gel filtration chromatography of a mixture of calibration proteins: conalbumin, ovalbumin, carbonic anhydrase and ribonuclease A. Pre, sample of conditioned media before gel filtration.

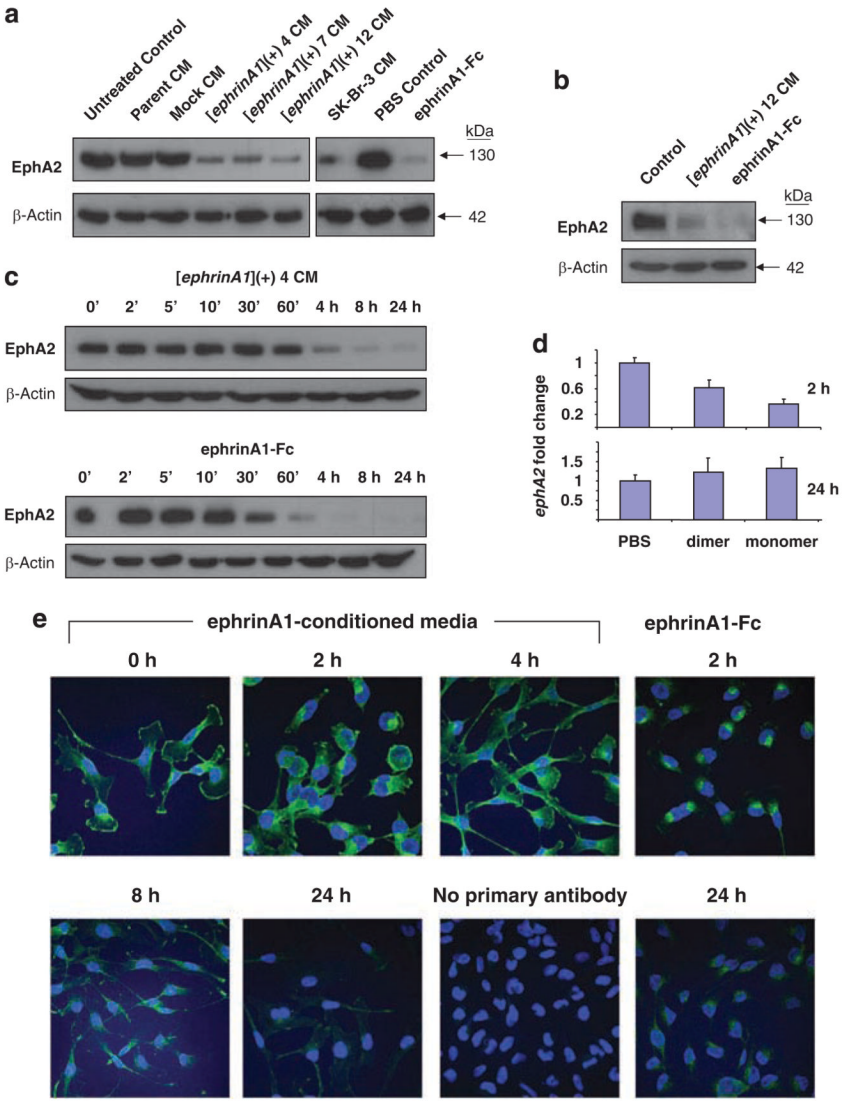

Figure 3.

Soluble monomeric ephrinA1 induces internalization and downregulation of EphA2. (**a**) Western blot analysis of EphA2 expression in U-251MG cells treated for 2 h with conditioned media (CM) from parent, empty-vector-transfected U-251[*ephrinA1*](+) 4, 7 or 12 cells, or SK-Br-3 cells, or with 1 μg/ml ephrinA1-Fc. (**b**) Western blot analysis of EphA2 expression in A-172MG cells treated for 24 h with U-251[*ephrinA1*](+) 12-conditioned media or 1 μg/ml ephrinA1-Fc. Control, cells treated with fresh growth media. (**c**) Western blot analysis of U-251MG cells treated for the indicated times with ephrinA1-conditioned media or 1 μg/ml ephrinA1-Fc. (**d**) real-time PCR analysis of *ephA2* in response to 2 or 24 h treatment with 1 μg/ml homodimeric ephrinA1-Fc or 4 μg/ml monomeric ephrinA1 generated by factor XA cleavage of ephrinA1-Fc. (**e**) Confocal microscopy of EphA2 immunofluoresence in U-251MG cells treated for the indicated times with ephrinA1-conditioned media or 1 μg/ml ephrinA1-Fc. All images were merged to visualize nuclei, which were stained with a DNA-binding probe, TO-PRO.

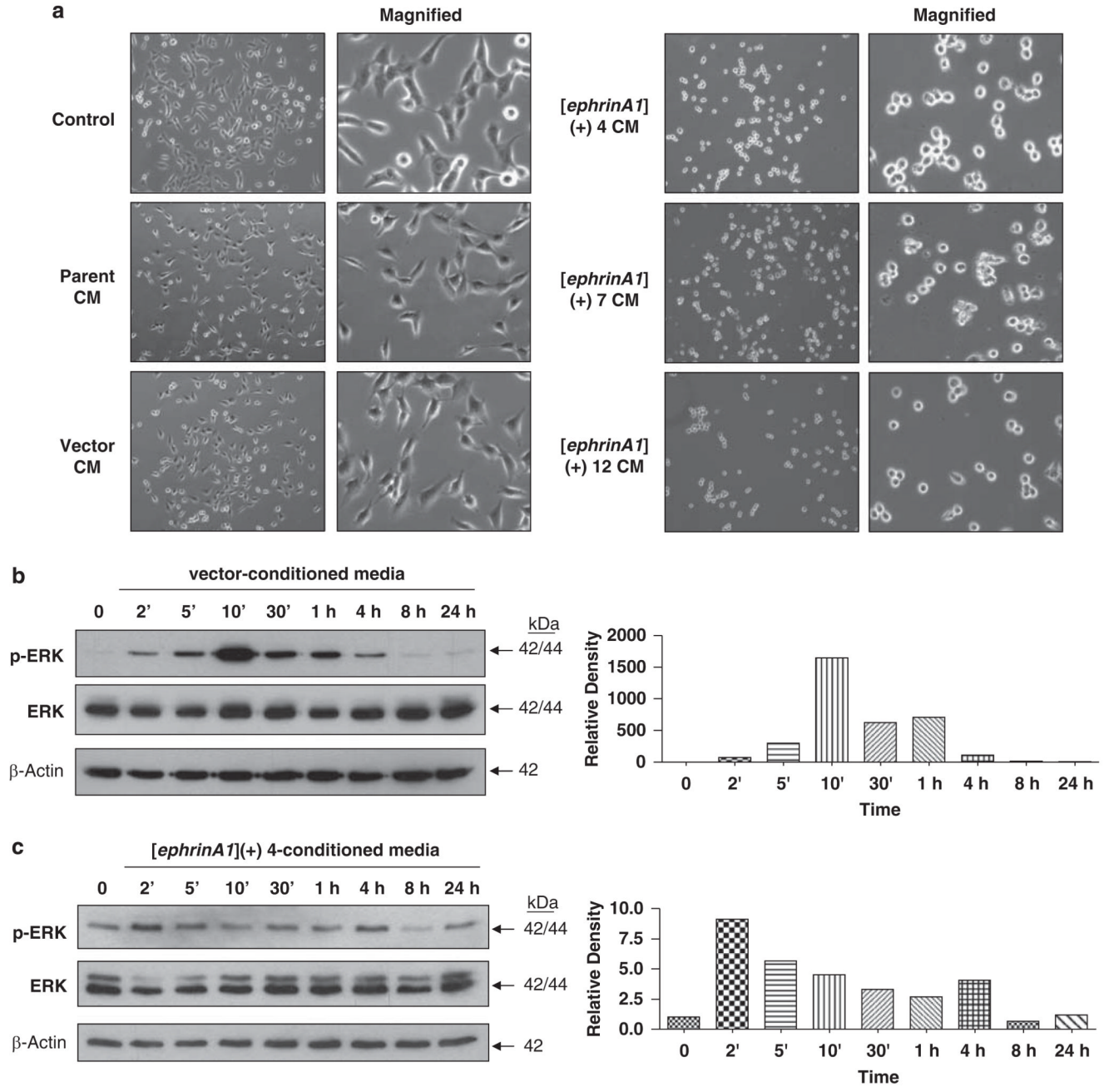

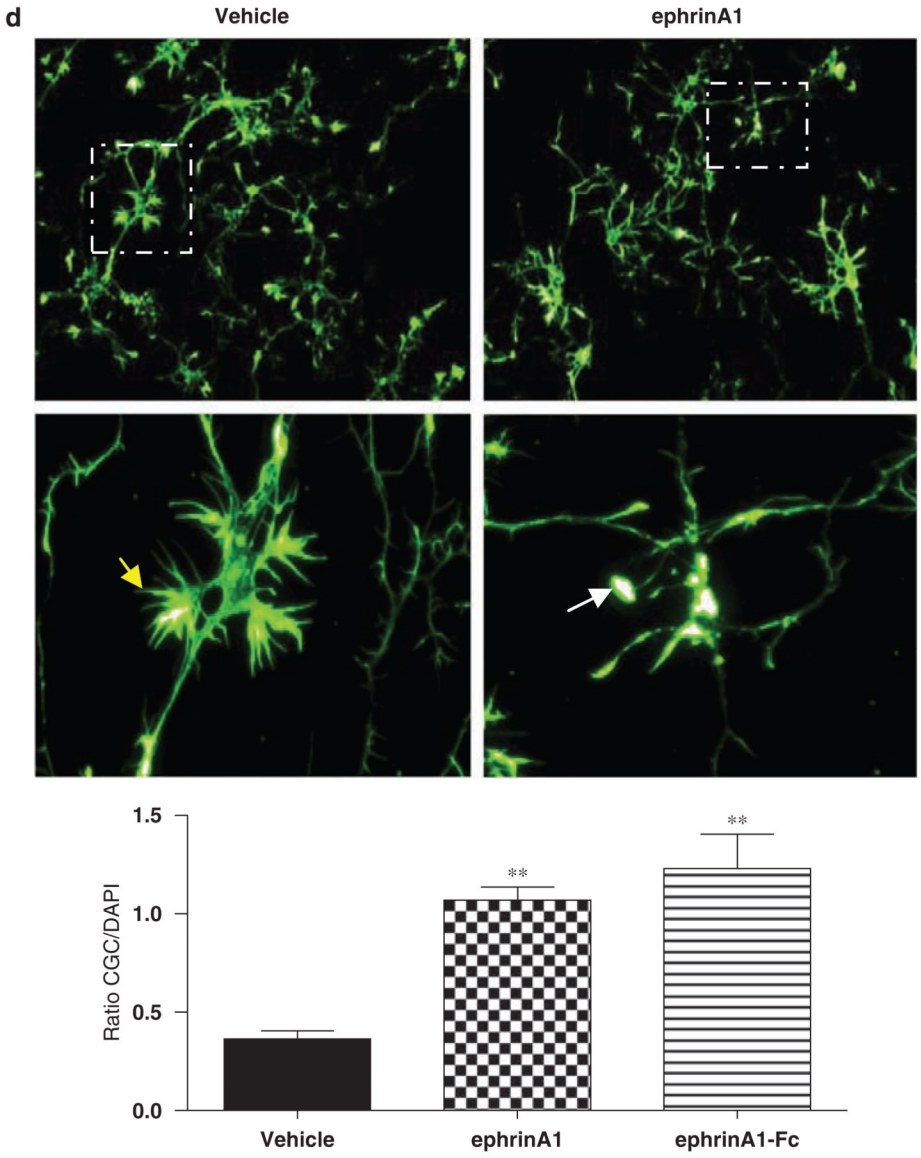

Figure 4.

Functional effects of soluble monomeric ephrinA1 in glioblastoma multiforme (GBM) cells and rat embryonic neurons. (**a**) Phase-contrast microscopy of U-251MG cells after treatment for 2 h with conditioned media (CM) obtained from parent, empty-vector-transfected or U-251[*ephrinA1*](+) 4, 7 and 12 cells. Control, untreated cells. Western blot analysis of phosphorylated Erk (p-ERK) and total Erk (ERK) protein in U-251MG cells treated with vector-conditioned media (**b**) or ephrinA1-conditioned media (**c**) for the indicated times. Densitometry corresponds to ERK normalized to β-actin, followed by p-Erk to ERK, which was then normalized to the control, cells at time=0. (**d**) Fluorescent images of primary embryonic rat cortical neurons stained for F-actin following treatment for 1 h with 1 μg/ml ephrinA1-Fc or monomeric ephrinA1 purified by gel filtration chromatography. Yellow arrows indicate areas of F-actin rich, expanded growth cones; white arrows indicate areas of collapsed growth cones. Collapsed neuronal growth cones were quantified and are graphically represented as the mean collapsed growth cones per cell number (CGC/DAPI) for each treatment group. ** P<0.001 vs vehicle.

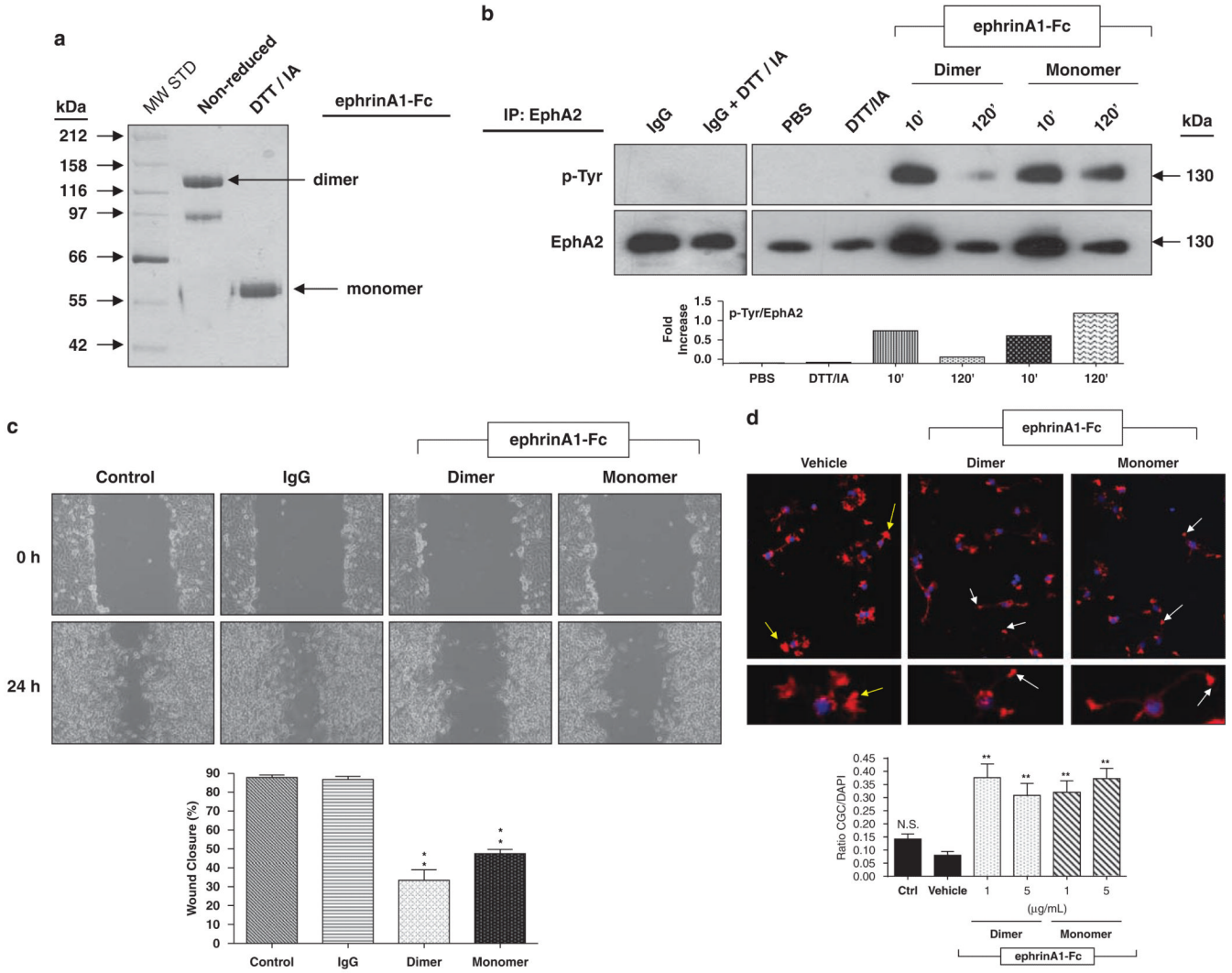

Figure 5.

Comparative analysis of the function of homodimeric and monomeric ephrinA1-Fc. (**a**) SDS–polyacrylamide gel electrophoresis analysis of non-reduced (NR) and reduced (R) ephrinA1-Fc showing the relative size of dimeric and monomeric ephrinA1-Fc used to treat U-251MG cells. S, molecular weight standards. (**b**) Phosphotyrosine (p-Tyr) and EphA2 detected by western blotting following immunoprecipitation with EphA2 in U-251MG cells treated with dimeric or monomeric ephrinA1-Fc or IgG, PBS, or the reducing/alkylating agents (DTT/IA). Densitometry analysis represents the fold increase of phosphorylated EphA2 compared to total EphA2. (**c**) Migration assay measuring the percent wound closure over time of U-251MG cells in the presence of 1 μg/ml dimeric or monomeric ephrinA1-Fc. **P*<0.001 vs IgG-treated cells. (**d**) Primary rat cortical neurons stained for F-actin following treatment for 1 h with 1 μg/ml of a dimer or monomer of ephrinA1-Fc or an equal volume of vehicle (phosphate-buffered saline (PBS)). Nuclei are stained with DAPI. Yellow arrows indicate areas of F-actin rich, expanded growth cones; white arrows indicate areas of collapsed growth cones. Collapsed neuronal growth cones were quantified and are graphically represented as the mean collapsed growth cones per cell number (CGC/DAPI) for each treatment group. ***P*<0.001 vs vehicle. Ctrl, non-treated cells.

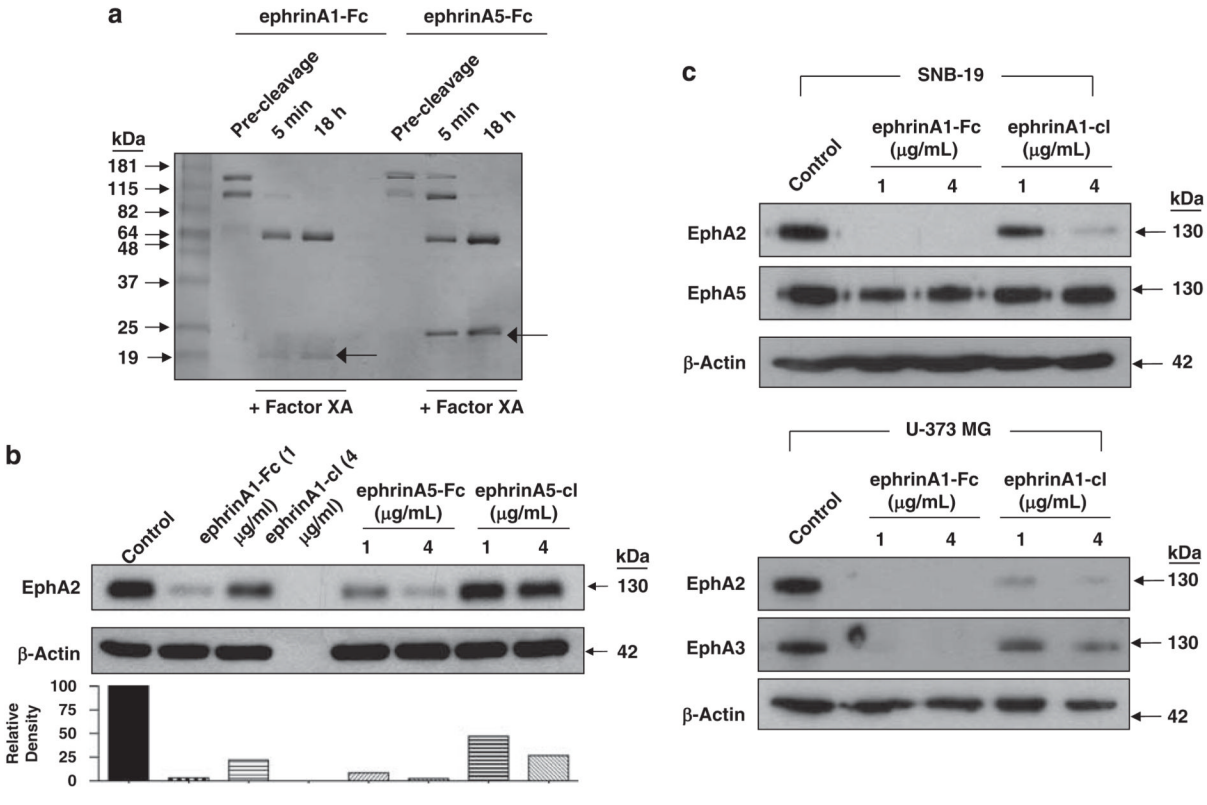

Figure 6.

Specificity of the Eph receptor–monomeric ephrin interaction. (**a**) SDS–polyacrylamide gel electrophoresis of Factor XA cleavage of ephrinA-Fc and ephrinA5-Fc. Shown are each of the proteins before treatment with enzyme (Pre-cleavage) and samples from the reaction at 5 min and 18 h after enzyme was added. (**b**) Western blot of EphA2 expression in U-251MG cells treated for 24 h with 1 μg/ml of ephrinA1-Fc, 4 μg/ml of the ephrinA1 Factor XA cleavage product (ephrinA1-cl) and 1 or 4 μg/ml of ephrinA5-Fc or the ephrinA5 Factor XA cleavage product (ephrinA5-cl). (**c**) Western blot of EphA2 and EphA5 expression in SNB-19 cells and EphA2 and EphA3 expression in U-373MG cells treated for 24 h with 1 or 4 μg/ml of ephrinA1-Fc or the ephrinA1 Factor XA cleavage product (ephrinA1-cl).

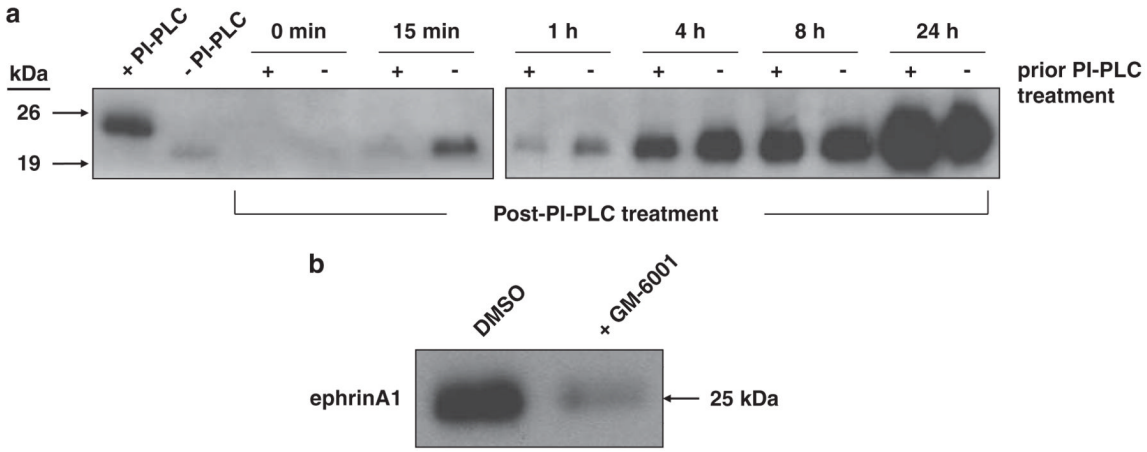

Figure 7.

Soluble ephrinA1 can be released from U-251MG cells by proteolytic cleavage. (**a**) Western blot analysis of ephrinA1 protein in conditioned media from U-251[*ephrinA1*](+) 12 cells after 20 min of treatment with PI-PLC (+ PI-PLC) or vehicle (−PI-PLC). Cells from each treatment group were then washed and fresh growth media added. At this time, a sample of media was collected (0′), and again at the indicated time points thereafter (15′–24 h). '+' represent samples from those cells previously treated with PI-PLC (+ PI-PLC), and '−' represent samples from those cells not previously treated with PI-PLC (−PI-PLC). (**b**) Western blot of ephrinA1 immunoreactivity in conditioned media 18 h after U-251[*ephrinA1*](+) cells were grown in the presence of 25 μM GM-6001 or an equal volume of dimethylsulfoxide (DMSO) (vehicle).